Effect of growth time on photoelectrochemical performance of TiO_2 nanotubes

Q. C. Abdulridha [a], A. M. Holi [a,*], A. Y. M. Al-Murshedi [b], A. A. Al-Zahrani [c]
[a] *Department of Physics, College of Education, University of Al-Qadisiyah, Al-Diwaniyah, Al-Qadisiyah 58002, Iraq*
[b] *Chemistry Department, College Education for Girls, Kufa University, An-Najaf, Iraq*
[c] *Imam Abdulrahman Bin Faisal University, Eastern Region, Dammam, Saudi Arabia*

This study investigates how the duration of anodization influences the structural and morphological characteristics and photoelectrochemical (PEC) performance of titanium dioxide (TiO_2) nanotube arrays (TNTs) fabricated via electrochemical anodic oxidation. Four different growth times, 0.5, 1, 1.5, and 2 hours, were tested to optimize the nanotubes' morphology and structure for PEC applications. X-ray diffraction (XRD) analysis confirmed the presence of the anatase phase across all samples, with increased phase intensity observed with longer anodization periods. Field emission scanning electron microscopy (FESEM) revealed that TNTs anodized for one hour exhibited a uniform, vertically aligned, and crack-free structure; however, extended anodization times introduced structural irregularities. Energy-dispersive X-ray spectroscopy (EDS) verified that all samples maintained a stoichiometric TiO_2 composition, with higher oxidation levels correlating with longer anodization durations. Diffuse reflectance spectroscopy (DRS) indicated a slight decrease in band gap energy as anodization time increased, implying enhanced visible-light absorption. Under illumination of 100 mW/cm², photoelectrochemical testing showed that TNTs anodized for one hour achieved the highest photocurrent density of 0.15 mA/cm² at 0 V vs. Ag/AgCl, with a corresponding photoconversion efficiency of 0.18%. These findings suggest that a one-hour anodization period produces TNTs with optimal structural and optoelectronic properties, making them highly suitable for efficient solar-driven water splitting and other PEC energy conversion technologies.

(Received June 30, 2025; Accepted September 9, 2025)

Keywords: Anodization method, TiO_2 nanotubes, Photoelectrochemical performance

1. Introduction

The transition to sustainable energy is necessary due to the expected depletion of fossil fuel reserves, the increasing instability of the energy supply, and the increasing cost of fossil fuels. The use of green and clean energy is on the rise as a result of environmental pollution and the growing global energies [1]. Photoelectrochemical cells (PEC cells) are therefore efficient in generating electrical energy from pure free solar radiation. It is generally agreed that the best solutions to the world's energy issues are sustainable energy conversion, consumption, and storage [2].Solar energy is the ideal renewable energy resource because it is abundant and readily available. In recent decades, semiconductors known as nanorods, nanowires, nanobelts, and nanotubes have been widely used in electrical and optoelectronic applications [3].

Due to their large surface area, nanostructures are particularly intriguing for photochemical applications because they are ideal for absorbing light and providing direct conduction channels for charge movement[4] . The photoanode, the most important component of PEC cells, is responsible for transporting photogenerated electrons to conductive substrates and loading light-absorbing materials. Currently, semiconductors are the most widely used photoanode materials. In addition to solar converters, semiconductors can be used as photocatalysts to remove

* Corresponding author: araa.holi@qu.edu.iq
https://doi.org/10.15251/JOR.2025.215.553

pollutants[5]. Scientists are interested in TiO_2 nanotube arrays (NTAs), a product of the anodic oxidation of titanium foils. These nanotubes may find application in solar cells, sensors, and PEC cells for hydrogen generation. The unique nanostructure of this semiconductor can improve the high charge collection efficiency due to its superior transport properties[6].

Optimal conversion processes are essential to efficiently convert solar energy into chemical and electrical energy. Greater emphasis should be placed on the development of functional electrode materials to ensure that photochemical cells operate as efficiently as possible. The integration of photocatalysis (PC) with electrochemical technology results in photoelectrochemical (PEC), a potent and efficient method for harnessing solar energy [7]. Following the advancement of the photoelectrochemical water-splitting technique utilizing a TiO_2 electrode, the TiO_2 photoelectrode has emerged as the most prevalent and promising alternative. It is cost-effective, ecologically sustainable, and chemically stable across diverse environments [8]. Based on the duration growth (anodization time) of the nanotubes, the visible-light band-gap shift and optimum structural uniformity are novel contributions in PEC systems. This work examines the influence of growth duration on the photoelectrochemical performance of TiO_2 nanotubes, drawing on foundational research on TiO_2-based photocatalytic systems. This may provide us with new insights into the utilization of water-splitting photoelectrochemical cells.

2. Experimental method

The titanium dioxide (TiO_2) nanotubes were fabricated using the anodization method, as shown in Scheme 1. Initially, the area (1 cm x 2.5 cm) pieces were cut from a 99.9% pure titanium foil sheet. These pieces were then cleaned through a washing process involving ultrasonic waves in solvents such as acetone, isopropanol, or deionized water for fifteen minutes, respectively. Then, the samples were soaked for 10 minutes in [6 M] HNO_3 to obtain a smooth surface. In the electrochemical cell, high-density graphite acted as the counter electrode, while the titanium foil served as the working electrode during anodization. The distance between the two electrodes was maintained at a fixed 2 centimeters. The anodization was carried out at 30 V, powered by a direct current supply (MP6010D) for one hour using an electrolytic solution (75 mL glycerin + 25 mL DIW + 0.5 g NH_4F). Then, the prepared samples were rinsed with DI water. Next, the samples were annealed for 2 hours in a furnace set at 500°C.

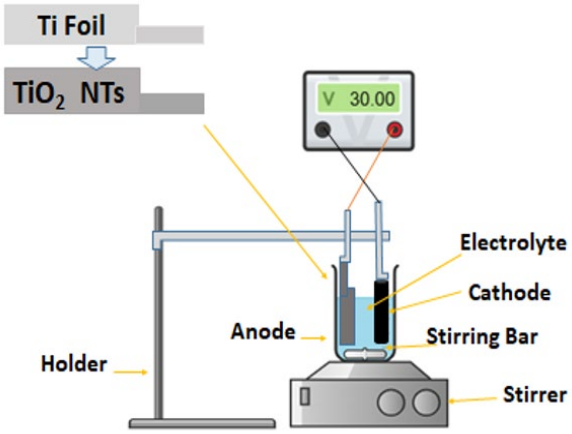

Scheme 1. Schematic diagram of anodization method setup.

The X-ray diffraction (XRD) analysis was performed using the Shimadzu LabX XRD-6000 diffractometer, which operated within a scanning range of 10º to 80º using Cu Kα radiation (λ = 1.54 Å). The instrument was set to an operating voltage of 40.0 kV and a current of 40.0 mA.

Morphological characterization of the samples was conducted through energy-dispersive X-ray spectroscopy (EDS) combined with a field-emission scanning electron microscope (Nova Nano SEM 450). UV-visible diffuse reflectance spectroscopy was carried out using the Shimadzu TM DUV 3700 double-beam spectrophotometer, covering a wavelength range from 200 to 800 nm. For photoelectrochemical (PEC) studies, a three-electrode electrochemical cell was constructed to evaluate the performance of TiO_2 for PEC applications. The working electrodes comprised TiO_2 nanotube (NT) samples, with a silver/silver chloride (Ag/AgCl) electrode serving as the reference, and a platinum (Pt) wire used as the counter electrode. The electrolyte solution was prepared by mixing 0.1 M Na_2SO_3 and 0.1 M Na_2S, resulting in a solution with a pH of approximately 13. TiO_2 NT samples with different growth durations served as the photoanodes. Photocurrent measurements were carried out using linear sweep voltammetry (LSV) on a Vertex One Potentiostat (Ivium Technologies, Netherlands), operated via IviumSoft software. The scans ranged between -1 V and +1 V versus Ag/AgCl at a scan rate of 20 mV/s. During illumination, a 120 V, 300 W halogen lamp was used to irradiate the quartz reaction cell, positioned 15 cm from the electrode surface, which had an active area of 1 cm^2. The light intensity was maintained at approximately 100 mW/cm^2 using manual chopping. The light intensity was measured using a fiberoptic spectrometer (Avaspec-2048). The photoconversion efficiency (η) of the TiO_2 nanotubes was calculated using the appropriate formula, taking into account the external bias applied to the PEC system to determine the bias photon-to-current efficiency (ABPE). When an external voltage was applied, electrical energy costs were deducted from the overall energy conversion considerations the applied bias photon-to-current efficiency (ABPE) is:

$$\boldsymbol{\eta = \frac{J_{ph}\left(E^{o}_{rev} - |E_{app.}|\right)}{P_{in}} \times 100\%} \qquad (1)$$

where P_{in} is the incident light irradiance (100 $mWcm^{-2}$), J_{ph} ($J_{ph} = J_L - J_D$) denotes the achieved photocurrent density (in $mAcm^{-2}$) under the externally applied voltage of V_{app} *vs.* Ag/AgCl. $E_{app.}$ denotes the standard reversible potential, which is 1.23 V vs. the normal hydrogen electrode (NHE), and E_{app} is the actual electrode potential between the working electrode and the counter electrode at which the photocurrent was measured under illumination [9].

3. Results and discussion

3.1. XRD analysis

The crystalline structures of titanium dioxide (TiO_2) nanotube arrays produced through varying anodization durations (0.5 h, 1 h, 1.5 h, and 2 h) were analyzed using X-ray diffraction (XRD). The diffraction patterns were compared to standard JCPDS cards: 00-044-1294 for metallic titanium (Ti) and 00-021-1272 for anatase TiO_2. As depicted in Figure 1, the untreated titanium substrate displayed prominent diffraction peaks at approximately 2θ = 35.42°, 38.6°, 40.44°, 53.52°, 63.15°, 70.8°, and 76.41°, which correspond to the (100), (002), (101), (102), (103), (112), and (201) planes of metallic Ti. After 0.5 hours of anodization (TNT0.5h), new peaks appeared at 2θ values of 25.11°, 38.23°, 47.86°, and 52.86°, associated with the (101), (004), (200), and (105) planes of anatase TiO_2, indicating the initial formation of crystalline anatase nanotubes. Extending the anodization to 1 hour (TNT1h) resulted in a sharper and more intense anatase (101) peak at around 25.3°, reflecting improved crystallinity and a preferred orientation along this thermodynamically stable plane. Simultaneously, the intensity of the metallic Ti peaks decreased, suggesting the development of a thicker and more uniform TiO_2 nanotube layer. At longer durations (1.5 h and 2 h), the anatase phase became even more pronounced, with additional peaks at 2θ = 62.8° and 75.8° corresponding to the (211) and (204) planes, respectively. These findings indicate ongoing crystalline growth and better structural order of the TiO_2 nanotubes with increasing anodization time. Throughout all samples, the anatase (101) peak remained the most prominent, underscoring its favored growth due to its low surface energy and high thermodynamic stability.

These results are in agreement with prior research [10–13]. The crystallite sizes were estimated using the Debye–Scherrer equation:

$$D = 0.9\lambda / \beta \cos\theta \quad (2)$$

where D is the crystallite size, λ is the X-ray wavelength (1.54 Å), β is the full width at half maximum (FWHM) of the (101) peak, and θ is the Bragg angle. For the sample anodized for 0.5 hours, the crystallite size was approximately 33.18 nm. When the anodization duration increased to 1 hour and 1.5 hours, the crystallite sizes decreased to 22.1 nm and 22.12 nm, respectively, indicating a refinement in nanostructure that enhances surface area and optical absorption. Interestingly, the sample anodized for 2 hours exhibited a larger crystallite size of 33.21 nm, similar to the 0.5-hour sample, with a corresponding FWHM of about 0.244. The broader diffraction peaks observed in the 1-hour and 1.5-hour samples (FWHM around 0.366) suggest improved crystal quality and smaller grain sizes compared to the 0.5-hour and 2-hour samples. These findings are consistent with previous research[14–16], which also indicated that intermediate anodization times tend to produce TiO_2 nanotubes with enhanced crystallinity and favorable structural properties.

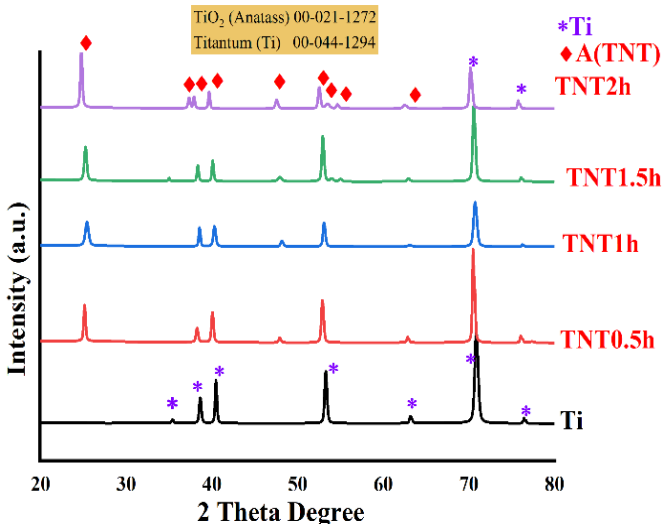

Fig. 1. XRD patterns are of the TNTs samples anodized for (0.5, 1, 1.5, 2) hours.

3.2. Morphological with EDS analysis

Figure 2 illustrates the significant differences in the morphology of titanium dioxide nanotubes (TiO_2 NTs) fabricated over varying time periods. The sample formed after 1 hour (TNT-1h) exhibited more orderly, aligned, and symmetrical nanotube structures, characterized by uniform and homogeneous dimensions with few defects. This suggests that a one-hour synthesis duration is optimal for producing TiO_2 nanotubes with superior structural qualities. In contrast, samples synthesized for shorter or longer times specifically 0.5 hours (TNT-0.5h), 1.5 hours (TNT-1.5h), and 2 hours (TNT-2h) appeared heterogeneous and displayed broken ends. The images reveal incomplete structures and irregular shapes in these samples compared to the 1-hour specimen. Such distortions and structural degradation could result from too brief a deposition period, which limits reaction time (as in TNT-0.5h), or from extended deposition periods, which lead to overexposure to the manufacturing conditions (as in TNT-1.5h and TNT-2h). To achieve the most uniform and high quality TiO_2 nanotubes, it is crucial to identify the optimal synthesis duration. The findings strongly support that a one-hour process yields well-structured, homogeneous, and aligned nanotubes with minimal defects[17,18].

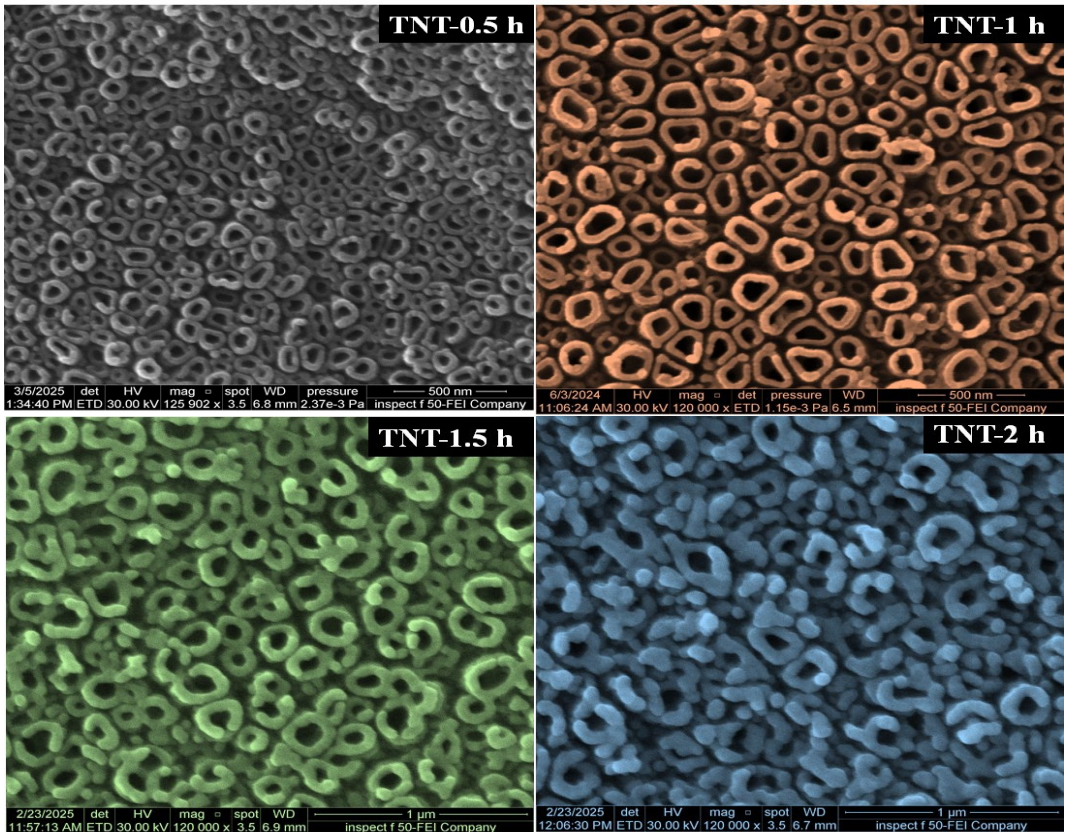

Fig. 2. FESEM images of the TNTs samples anodized for (a. 0.5, b. 1, c. 1.5, d. 2) hours.

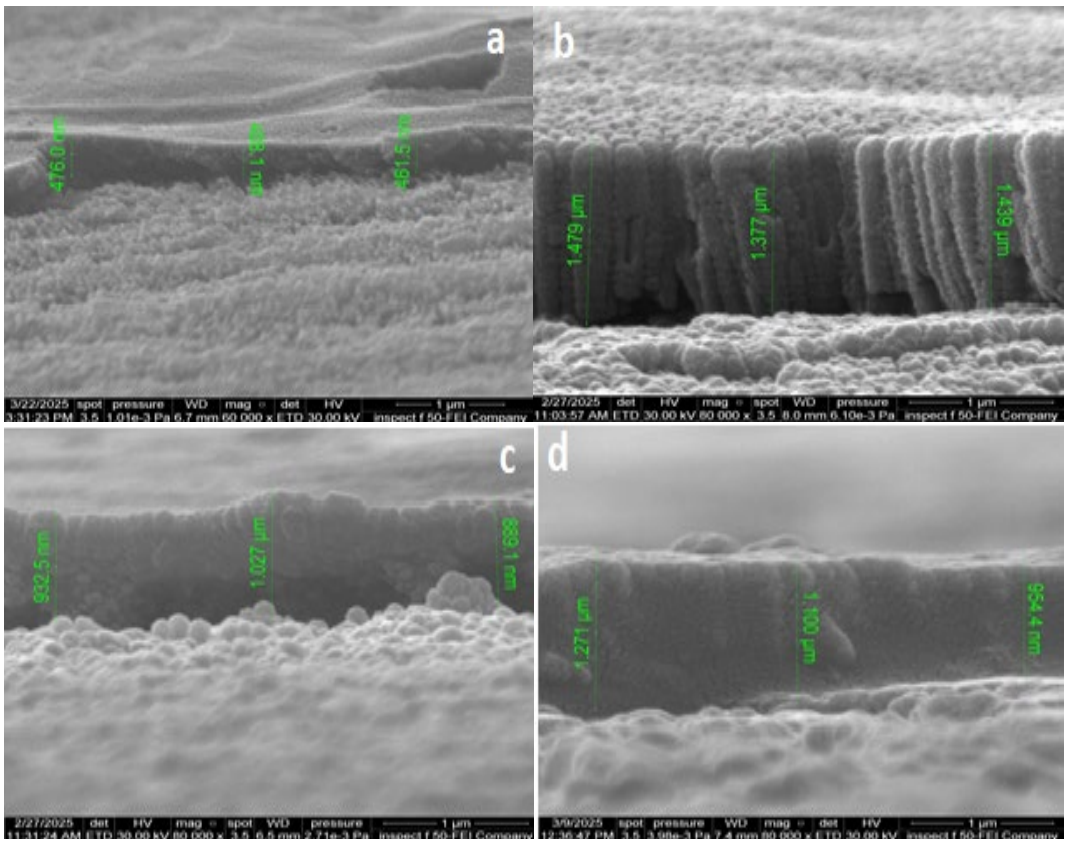

Fig. 3. Cross-section images of the TNTs samples anodized for (a. 0.5, b. 1, c. 1.5, d. 2) hours.

The duration of the fabrication process influences the morphology of the nanotubes, as depicted in images (a), (b), (c), and (d) of Figure 3. Longer fabrication times lead to changes in structural density and shape, as evidenced by the cross-section images. At half an hour post-deposition, image (a) shows that the nanotubes are incomplete at the ends, relatively short, and exhibit poor surface uniformity, with gaps between them. After one hour of deposition, the nanotubes appear more uniform, orderly, and aligned, with increased length, indicating enhanced growth or interaction and suggesting an improvement in structural and morphological properties as seen in image (b). At one and a half hours, the nanotubes form more cohesive structures with higher density, though they are shorter compared to the one-hour mark, as seen in image (c). After two hours, the nanotubes seem to reach a more stable phase, characterized by a thicker, more compact structure in image (d). This progression may be attributed to the extended catalytic time, which facilitates the formation of denser layers or additional structural features[19].

Energy-dispersive X-ray spectroscopy (EDS) analysis, illustrated in Figure 4, reveals the elemental composition and relative weight and atomic percentages of titanium (Ti) and oxygen (O) in the TiO_2 nanotube arrays formed at different anodization durations. The tabulated data within each image indicates a clear trend in oxygen incorporation over time. At a deposition duration of 0.5 hours, the oxygen concentration is rather low, indicating incomplete oxidation and an inadequately formed TiO_2 layer. This outcome indicates that the nanotube production process remains nascent, characterized by inadequate oxygen absorption to establish a distinct oxide layer. Extending the anodization to one-hour results in a substantial rise in oxygen content, attaining 12.9% by weight and 30.7% by atomic percentage. This signifies a significant enhancement in oxide synthesis, suggesting the emergence of a more stoichiometric and homogeneous TiO_2 layer. An additional extension to 1.5 hours yields a marginal increase in oxygen content to 13.3% by weight and 31.5% by atomic percentage. This improvement indicates that the oxidation process is nearing equilibrium, with the nanotube arrays almost fully formed and attaining ideal stoichiometry. At the 2-hour mark, a little reduction in oxygen content is noted (12.1% by weight and 29.3% by atomic percentage), alongside a relative increase in titanium content. This reduction may indicate the onset of surface restructuring, degradation, or partial dissolution of the oxide layer, potentially due to prolonged exposure to the electrolyte under oxidative conditions. These findings are consistent with those of the researchers [20–23]. These compositional shifts emphasize that a (1–1.5) hour anodization duration yields the most chemically balanced and stable TiO_2 nanotube structure, aligning with morphological and crystallographic observations.

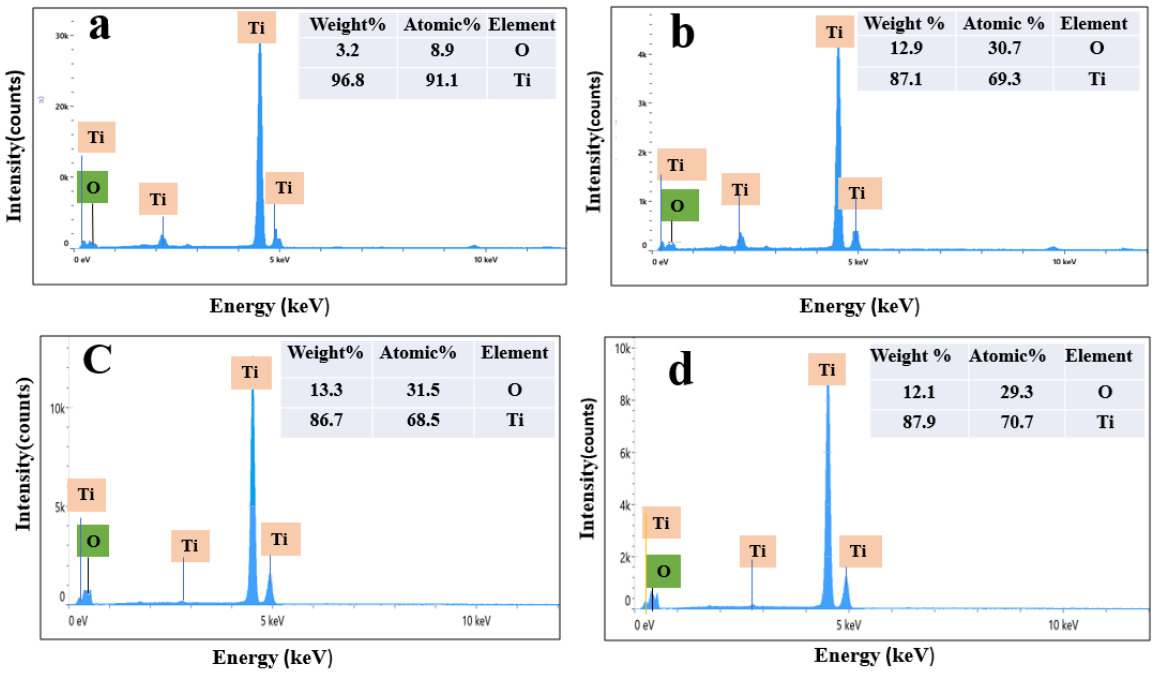

Fig. 4. Energy-dispersive X-ray spectra of the TNTs samples anodized for (a. 0.5, b. 1, c. 1.5, d. 2) hours.

3.3. UV-Vis (DRS) analysis

The optical characteristics of the prepared samples were examined using DRS technique, as shown in Figure 5. All samples showed notable absorption in the UV area due to the inherent optical absorption properties of TiO_2, with absorption edges often seen between 350 and 400 nm, which is a property of TiO_2. This suggests the presence of anatase or a mixed-phase TiO_2 structure, consistent with previous studies [24–27]. The Tauc equation was used to estimate the band gaps of the four samples [28].

$$(\alpha h\nu)^n = h\nu - Eg \tag{3}$$

where: α is the absorption coefficient, $h\nu$ is the photon energy, and E_g is the optical band gap. $n = 2$ for direct band gap. The optical band gap (E_g) is determined by extrapolating the linear segment of the curve to zero. The Tauc plot indicates that the samples anodized for varying durations have varied band gaps, measured at $3.32\ eV$, $3.20\ eV$, $3.16\ eV$, and $3.10\ eV$ are shown in Figure 6. Following an increase times deposition, the band gap is somewhat displaced into the visible spectrum. The differing band gap values arise from nanotube structures linked to diverse morphologies resulting from variable anodization times. An extended anodization duration results in a systematic redshift of the absorption edge, signifying a reduction in the optical band gap. This alteration may be ascribed to multiple variables, such as augmented nanotube length, enhanced crystallinity, and improved light scattering resulting from modifications in surface morphology and tube wall thickness. Extended anodization results in thicker oxide layers and elongated tubes, so increasing the light path and augmenting absorption, especially in the near-visible spectrum. The redshift in the absorption edge may be linked to the diminishing influence of quantum confinement effects as the nanotubes lengthen and their diameter expands. Moreover, extended growth durations may create oxygen vacancies and Ti^{3+} defect states inside the band structure, thereby affecting the optical absorption properties. These UV-Vis spectra trends are consistent with earlier findings. Mor et al., for instance, showed that longer anodization times result in longer tubes and more surface area, which improves the effectiveness of light harvesting [29]. Similarly, by adjusting anodization parameters like voltage and duration, Yahya et al., demonstrated the tunability of TNTs' electrical and optical characteristics [30]. The ability to manipulate the optical absorption of TNTs through anodization time is particularly significant for applications in photocatalysis and photoelectrochemical water splitting, where enhanced light absorption can directly contribute to improved performance within the visible spectrum, and this is consistent with earlier research [31–35].

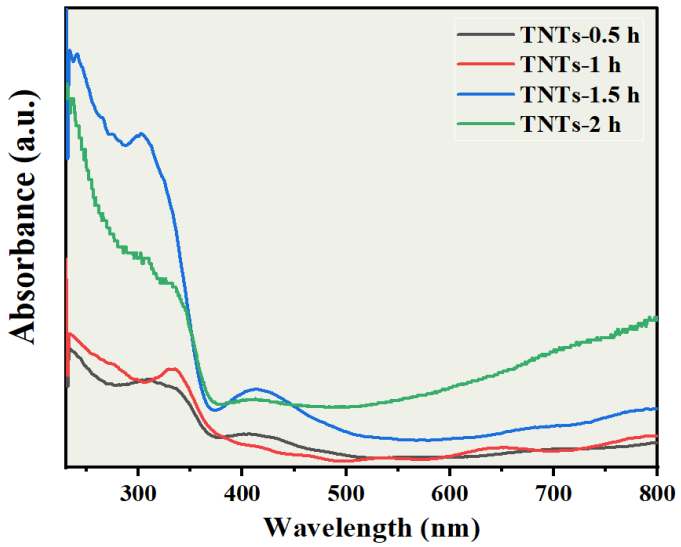

Fig. 5. UV – Vis (DRS) spectra of the TNTs samples anodized for (0.5, 1, 1.5, 2) hours.

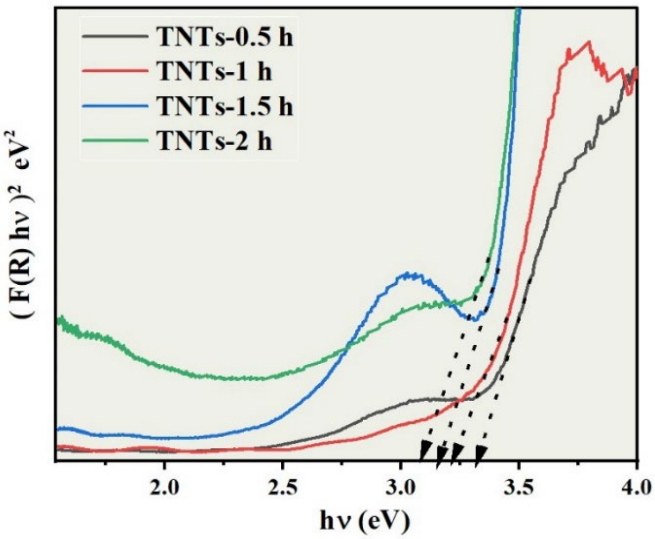

Fig. 6. UV – Vis (DRS) spectra of the TNTs samples anodized for (0.5, 1, 1.5, 2) hours.

3.4. Photoelectrochemical performance

Figure 7 presents J–V characteristics of different growth durations of TiO_2 nanotubes (TNT) photoanodes measured under illumination, illustrating their photoelectrochemical response. In all samples, the photocurrent density increases with more positive applied potentials, demonstrating photoanodic behavior characteristic of n-type semiconductors such as TiO_2. This trend is attributed to the enhanced collection of photogenerated holes at higher bias voltages. Notably, the photocurrent onset the point at which the current begins to increase significantly is consistent across all curves, indicating that the band edge positions remain largely unaffected by variations in the growth duration. At higher applied potentials (typically >0.6 V vs. Ag/AgCl), the photocurrent response tends to saturate, suggesting that either surface reaction kinetics or charge transport limitations dominate the overall performance. Samples with shorter growth durations exhibit relatively low photocurrent densities, which can be ascribed to incomplete crystallization, a higher density of structural defects or trap states within the nanotube walls, and limited carrier mobility. In contrast, an optimal growth duration yields the highest photocurrent density, reflecting improved charge separation efficiency, superior crystallinity, and a balanced nanotube geometry that supports effective transport and interfacial charge transfer. However, overextended growth durations appear to degrade performance, likely due to excessive grain growth, which reduces surface area formation of recombination centers at grain boundaries, or even collapse and sintering of the nanotube architecture. The photoconversion efficiency (η) of TiO_2 nanotube arrays (TNTs) anodized for different durations was evaluated under illumination at 0 V vs. Ag/AgCl. The calculated efficiencies were 0.11%, 0.18%, 0.15%, and 0.14% for the 0.5 h, 1 h, 1.5 h, and 2 h anodized samples, respectively, Table 1. Among the samples, the 1 h-TNTs exhibited the highest photoconversion efficiency of 0.18%, which can be attributed to an optimal sample for nanotube length. At this stage of anodization, the TNTs likely provide sufficient surface area for light absorption and active sites for water oxidation, while still maintaining efficient electron transport pathways with minimal recombination losses. In contrast, the 0.5 h-TNTs displayed the lowest efficiency (0.11%), likely due to insufficient nanotube growth, resulting in reduced surface area and poor light harvesting. Although longer anodization times (1.5 h and 2 h) led to the formation of longer TNTs, the marginal decline in efficiency suggests that excessively long nanotubes might introduce increased charge transport resistance and enhanced recombination due to longer electron diffusion paths. These results highlight the importance of optimizing anodization duration to balance light absorption, charge separation, and charge transport properties. Specifically, shorter anodization times help prevent structural irregularities and maintain stoichiometry, while band-gap narrowing enhances visible-light absorption. The observed trends demonstrate that morphological and structural tuning of TNTs through precise control of anodization time is a key factor in

maximizing PEC performance for water-splitting applications, offering improvements over previously reported studies [36–39].

Table 1. Photoconversion efficiency (η) of TiO_2 nanotube arrays (TNTs) anodized for different durations.

Sample	J_{ph} (mA/cm²) @ 0 V	η (%)
0.5 h-TNTs	0.09	0.11
1 h-TNTs	0.15	0.18
1.5 h-TNTs	0.13	0.15
2 h-TNTs	0.12	0.14

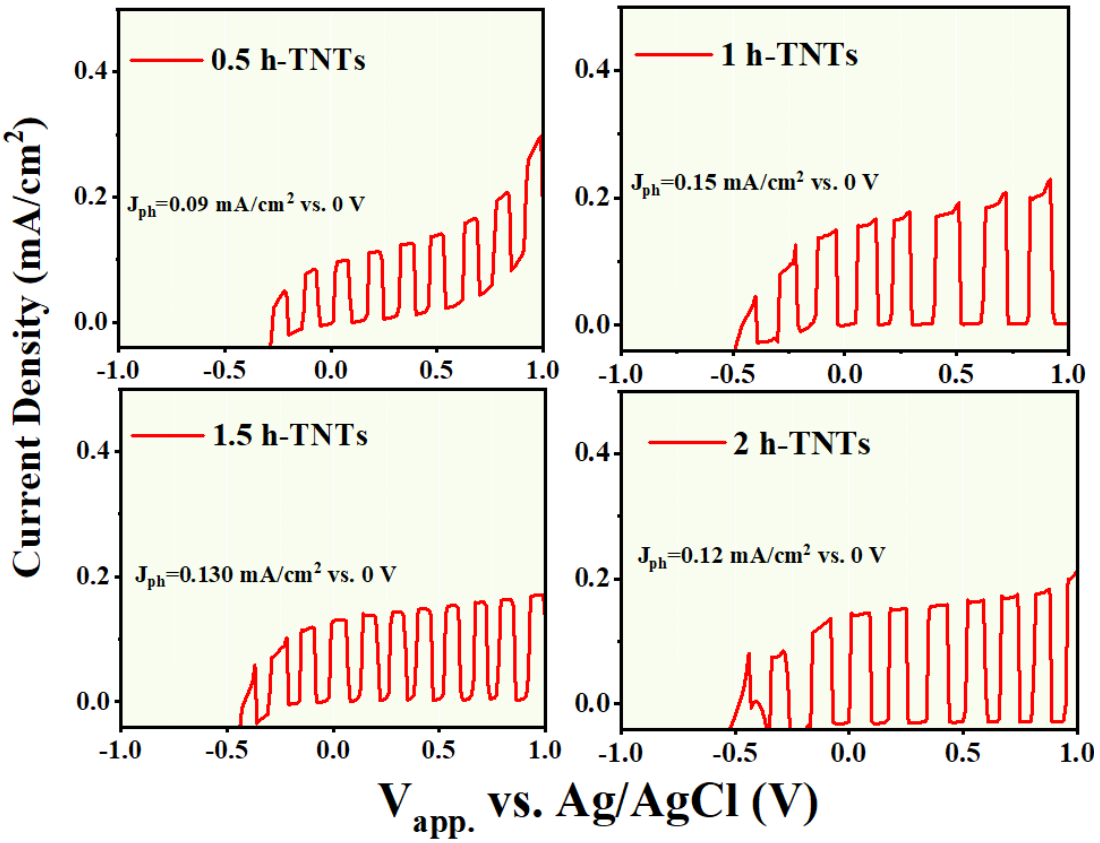

Fig. 7. Linear sweep voltammograms obtained at the scan rate of 20 mV s^{-1} at applied potentials from –1 to 1 V under illumination intensity of 100 mW cm^{-2} in 0.1 M Na_2S and Na_2SO_3 electrolyte for plain TiO_2 NTs of (a) 0.5 h (b) 1 h (c) 1.5 h (d) 2h.

4. Conclusion

The anodization duration is a decisive factor in tailoring the structural, morphological, optical, and photoelectrochemical characteristics of TiO_2 nanotube arrays. Among the various synthesis durations investigated, a 1-hour anodization time yielded nanotubes with the most advantageous balance of properties, including uniform and vertically aligned morphology, enhanced crystallinity, an appropriate band gap favoring visible-light absorption, and a markedly higher photocurrent response. These synergistic features render the 1-hour anodized TNTs highly suitable for photoelectrochemical applications such as solar energy conversion and environmental remediation. In contrast, both shorter and longer anodization periods were found to induce morphological irregularities, limit charge transfer, or impair light-harvesting capability, thereby reducing overall PEC performance. Consequently, the 1-hour anodization time can be considered

optimal for achieving multifunctional performance. Future investigations directed at fine-tuning parameters such as applied voltage, electrolyte composition, and post-synthesis treatments are expected to further optimize the properties and expand the applicability of TiO_2 nanotube systems in advanced renewable energy technologies.

Acknowledgments

The authors gratefully acknowledge the support provided by the University of Al-Qadisiyah, the University of Kufa, and Imam Abdulrahman Bin Faisal University for facilitating this research. Their contribution in terms of laboratory access, technical support, and academic collaboration was instrumental in the successful completion of this study.

Conflict of interest

The authors declare no conflicting of interest.

References

[1] Abd Aziz, Azrina, International Journal of Engineering Technology and Sciences 5, no. 3 (2018): 132-139; https://doi.org/10.15282/ijets.v5i3.1136

[2] Allen, Norman S., Noredine Mahdjoub, Vladimir Vishnyakov, Peter J. Kelly, Roelof J. Kriek, Polymer degradation and stability 150 (2018): 31-36; https://doi.org/10.1016/j.polymdegradstab.2018.02.008

[3] Hreo, Hawraa Sabah, Araa Mebdir Holi, Asla Abdullah Al-Zahrani, Asmaa Kadim Ayal, M. R. Almamari, Bulletin of Materials Science 45, no. 4 (2022): 205; https://doi.org/10.1007/s12034-022-02781-7

[4] Xu, Yin, Giovanni Zangari, Coatings 11, no. 8 (2021): 931; https://doi.org/10.3390/coatings11080931

[5] Budiman, Harry, Rahmat Wibowo, Oman Zuas, and Jarnuzi Gunlazuardi, EduChemia: Jurnal Kimia dan Pendidikan 6, no. 2 (2021): 159-171; https://doi.org/10.30870/educhemia.v6i2.10793

[6] Guan, Dongsheng, Ying Wang, Nanoscale 4, no. 9 (2012): 2968-2977; https://doi.org/10.1039/c2nr30315a

[7] Yoo, Hyeonseok, Moonsu Kim, Yong-Tae Kim, Kiyoung Lee, Jinsub Choi, Catalysts 8, no. 11 (2018): 555; https://doi.org/10.3390/catal8110555

[8] Regonini, Domenico, Chris R. Bowen, Angkhana Jaroenworaluck, Ron Stevens, Materials Science and Engineering: R: Reports 74, no. 12 (2013): 377-406; https://doi.org/10.1016/j.mser.2013.10.001

[9] Al-Zahrani, Asla Abdullah, Zulkarnain Zainal, Zainal Abidin Talib, Hong Ngee Lim, Araa Mebdir Holi, Noor Nazihah Bahrudin, Arabian Journal of Chemistry 13, no. 12 (2020): 9166-9178; https://doi.org/10.1016/j.arabjc.2020.10.040

[10] Díaz-Real, Jesús A., Geyla C. Dubed-Bandomo, Juan Galindo-de-la-Rosa, Luis G. Arriaga, Janet Ledesma-García, Nicolas Alonso-Vante, Beilstein Journal of Nanotechnology 9, no. 1 (2018): 2628-2643; https://doi.org/10.3762/bjnano.9.244

[11] Yi, Zao, Yu Zeng, Hui Wu, Xifang Chen, Yunxia Fan, Hua Yang, Yongjian Tang, Yougen Yi, Junqiao Wang, Pinghui Wu, Results in Physics 15 (2019): 102609; https://doi.org/10.1016/j.rinp.2019.102609

[12] Altomare, Marco, Michele Pozzi, Mattia Allieta, Luca Giacomo Bettini, Elena Selli, Applied Catalysis B: Environmental 136 (2013): 81-88; https://doi.org/10.1016/j.apcatb.2013.01.054

[13] Ye, Liqun, Jin Mao, Jinyan Liu, Zhuo Jiang, Tianyou Peng, Ling Zan, Journal of Materials

Chemistry A 1, no. 35 (2013): 10532-10537; https://doi.org/10.1039/c3ta11791j

[14] Ahmed, Faheem, Syed A. Pervez, Abdullah Aljaafari, Adil Alshoaibi, Hatem Abuhimd, JooHyeon Oh, Bon Heun Koo, Micromachines 10, no. 11 (2019): 742; https://doi.org/10.3390/mi10110742

[15] Paul, Tapash Chandra, Jiban Podder, Applied Physics A 125, no. 12 (2019): 818; https://doi.org/10.1007/s00339-019-3112-9

[16] Macak, Jan M., Hiroaki Tsuchiya, Andrei Ghicov, Kouji Yasuda, Robert Hahn, Sebastian Bauer, Patrik Schmuki, Current Opinion in Solid State and Materials Science 11, no. 1-2 (2007): 3-18; https://doi.org/10.1016/j.cossms.2007.08.004

[17] Jedi-soltanabadi, Zahra, Negin Pishkar, Mahmood Ghoranneviss, Journal of Theoretical and Applied Physics 12 (2018): 135-139; https://doi.org/10.1007/s40094-018-0290-3

[18] Yin, Bo, Qun Qian, Zhongliang Xiong, Hongyi Jiang, Yue Lin, Daolun Feng, Nanotechnology 30, no. 15 (2019): 155702; https://doi.org/10.1088/1361-6528/aafd54

[19] Ge, Mingzheng, Qingsong Li, Chunyan Cao, Jianying Huang, Shuhui Li, Songnan Zhang, Zhong Chen, Keqin Zhang, Salem S. Al-Deyab, Yuekun Lai, Advanced science 4, no. 1 (2017): 1600152; https://doi.org/10.1002/advs.201600152

[20] Zhang, Junmeng, Jianmin Lu, Panzhe Hou, Yujie Liu, Zixuan Li, Peipei Lu, Guangyu Wen, Lihu Liu, Huiyuan Sun, Journal of Alloys and Compounds 952 (2023): 170010; https://doi.org/10.1016/j.jallcom.2023.170010

[21] Khan, M. Alam, Hee-Tae Jung, O-Bong Yang, The Journal of Physical Chemistry B 110, no. 13 (2006): 6626-6630; https://doi.org/10.1021/jp057119k

[22] Xie, Yibing, Chen Yao, Materials Research Express 6, no. 12 (2020): 125550; https://doi.org/10.1088/2053-1591/ab69c9

[23] Hsu, Ming-Yi, Wei-Chun Yang, Hsisheng Teng, Jihperng Leu, Journal of The Electrochemical Society 158, no. 3 (2011): K81; https://doi.org/10.1149/1.3533388

[24] Mishra, Vikash, M. Kamal Warshi, Aanchal Sati, Anil Kumar, Vinayak Mishra, Rajesh Kumar, P. R. Sagdeo, SN Applied Sciences 1 (2019): 1-8; https://doi.org/10.1007/s42452-019-0253-6

[25] Ge, Ming-Zheng, Shu-Hui Li, Jian-Ying Huang, Ke-Qin Zhang, Salem S. Al-Deyab, Yue-Kun Lai, Journal of Materials Chemistry A 3, no. 7 (2015): 3491-3499; https://doi.org/10.1039/C4TA06354F

[26] Valeeva, A. A., E. A. Kozlova, A. S. Vokhmintsev, R. V. Kamalov, I. B. Dorosheva, A. A. Saraev, I. A. Weinstein, A. A. Rempel, Scientific reports 8, no. 1 (2018): 9607; https://doi.org/10.1038/s41598-018-28045-1

[27] López, Rosendo, Ricardo Gómez, Journal of sol-gel science and technology 61 (2012): 1-7; https://doi.org/10.1007/s10971-011-2582-9

[28] Makuła, Patrycja, Michał Pacia, Wojciech Macyk, The Journal of Physical Chemistry Letters 9, no. 23 (2018): 6814-6817; https://doi.org/10.1021/acs.jpclett.8b02892

[29] Mor, Gopal K., Oomman K. Varghese, Maggie Paulose, Karthik Shankar, Craig A. Grimes, Solar Energy Materials and Solar Cells 90, no. 14 (2006): 2011-2075; https://doi.org/10.1016/j.solmat.2006.04.007

[30] Alivov, Yahya, Vladimir Kuryatkov, Mahesh Pandikunta, Gautam Rajanna, Daniel Johnstone, Ayrton Bernussi, Sergey A. Nikishin, Z. Y. Fan, MRS Online Proceedings Library (OPL) 1178 (2009): 1178-AA09; https://doi.org/10.1557/PROC-1178-AA09-27

[31] Díaz-Real, Jesús A., Geyla C. Dubed-Bandomo, Juan Galindo-de-la-Rosa, Luis G. Arriaga, Janet Ledesma-García, Nicolas Alonso-Vante, Beilstein Journal of Nanotechnology 9, no. 1 (2018): 2628-2643; https://doi.org/10.3762/bjnano.9.244

[32] Hu, Jinghua, Shiwu Hu, Yingping Yang, Shengqiang Tong, Jiejie Cheng, Mengwei Chen, Li Zhao, Jinxia Duan, International Journal of Photoenergy 2016, no. 1 (2016): 4651654; https://doi.org/10.1155/2016/4651654

[33] Regonini, D., F. J. Clemens, Materials Letters 142 (2015): 97-101; https://doi.org/10.1016/j.matlet.2014.11.145

[34] Qin, Lianjie, Qijing Chen, Ruijun Lan, Runqian Jiang, Xiao Quan, Bin Xu, Feng Zhang, Yongmin Jia, Journal of Materials Science & Technology 31, no. 10 (2015): 1059-1064; https://doi.org/10.1016/j.jmst.2015.07.012

[35] Ayal, Asmaa Kadim, Al-Mustansiriyah Journal of Science 29, no. 3 (2019): 77-81; https://doi.org/10.23851/mjs.v29i3.640

[36] Ansón-Casaos, Alejandro, José Carlos Ciria, Carlos Martínez-Barón, Belén Villacampa, Ana M. Benito, Wolfgang K. Maser, International Journal of Hydrogen Energy 52 (2024): 1146-1158; https://doi.org/10.1016/j.ijhydene.2023.06.284

[37] Song, Jingnan, Maojun Zheng, Xiaoliang Yuan, Qiang Li, Faze Wang, Liguo Ma, Yuxiu You et al., Journal of Materials Science 52 (2017): 6976-6986; https://doi.org/10.1007/s10853-017-0930-z

[38] Matsuda, Atsunori, Srimala Sreekantan, Warapong Krengvirat, Journal of Asian Ceramic Societies 1, no. 3 (2013): 203-219; https://doi.org/10.1016/j.jascer.2013.07.001

[39] Cho, Hyekyung, Hyunku Joo, Hansung Kim, Ji-Eun Kim, Kyoung-Soo Kang, Jaekyung Yoon, Chemosphere 267 (2021): 129289; https://doi.org/10.1016/j.chemosphere.2020.129289